

AD 730906

COPY NO. 27



PICATINNY ARSENAL TECHNICAL REPORT 4255
THE GRUNEISEN CONSTANT
OF
POROUS MATERIALS
IN
ENERGY DEPOSITION MATERIALS

BY
PAUL HARRIS

AUGUST 1971

APPROVED FOR PUBLIC RELEASE: DISTRIBUTION UNLIMITED.

PICATINNY ARSENAL
DOVER, NEW JERSEY

Prepared by
NATIONAL TECHNICAL
INFORMATION SERVICE
1701 J. W. WALKER BLVD.
SPRINGFIELD, VA 22151

DDC
RECEIVED
14 1971
C

28

UNCLASSIFIED

Security Classification

DOCUMENT CONTROL DATA - R&D		
<i>(Security classification of title, body of abstract and indexing annotation must be entered when the overall report is classified)</i>		
1. ORIGINATING ACTIVITY (Corporate author) U.S. Army, Picatinny Arsenal, Dover, New Jersey 07891	2a. REPORT SECURITY CLASSIFICATION Unclassified	2b. GROUP
3. REPORT TITLE THE GRUNEISEN CONSTANT OF POROUS MATERIALS IN ENERGY DEPOSITION MATERIALS (U)		
4. DESCRIPTIVE NOTES (Type of report and inclusive dates) Detailed proposal that usual energy deposition and the usual shock introduction do not yield a true Gruneisen parameter of porous matter.		
5. AUTHOR(S) (Last name, first name, initial) Harris, Paul		
6. REPORT DATE August 1971	7a. TOTAL NO. OF PAGES 28	7b. NO. OF REFS 21
8a. CONTRACT OR GRANT NO. N/A	8c. OPERATOR'S REPORT NUMBER(S) Picatinny Arsenal Technical Report 4255	
8. PROJECT NO. N/A	9. OTHER REPORT NO(S) (Any other numbers that may be assigned this report)	
10. AVAILABILITY/LIMITATION NOTICES Approved for public release; distribution unlimited.		
11. SUPPLEMENTARY NOTES	12. SPONSORING MILITARY ACTIVITY Picatinny Arsenal, Dover, N. J. 07801	
13. ABSTRACT <p>It is proposed that the usual energy deposition, e.g., electron beam, experiments, as well as the usual shock introduction, e.g., flyer plate, experiments do not yield a true Gruneisen parameter of porous materials. It is proposed that in a porous material stress relief occurs within the time that energy is being deposited, or before the final state is reached in a flyer plate experiment. Both types of experiments are analyzed and correlated and agree with the ideas put forward here. Energy deposition experiments of Shea, Mazella, and Avrami (porous PETN), and flyer plate experiments of Boade (sintered porous copper), are considered.</p> <p>Wave propagation in porous materials is considered in some detail, and it is concluded that in such materials macroscopic measurements can not always be used to determine microscopic parameters. It is proposed that a porous material acts as a diffraction grating with respect to a shock wave, and that unidirectional one-dimensional strain does not hold.</p>		

DD FORM 1473
JAN 64

UNCLASSIFIED
Security Classification

	LINK A		LINK B		LINK C	
	ROLE	WT	ROLE	WT	ROLE	WT

INSTRUCTIONS

1. ORIGINATING ACTIVITY: Enter the name and address of the contractor, subcontractor, grantee, Department of Defense activity or other organization (*corporate author*) issuing the report.

2a. REPORT SECURITY CLASSIFICATION: Enter the overall security classification of the report. Indicate whether "Restricted Data" is included. Marking is to be in accordance with appropriate security regulations.

2b. GROUP: Automatic downgrading is specified in DoD Directive 5200.10 and Armed Forces Industrial Manual. Enter the group number. Also, when applicable, show that optional markings have been used for Group 3 and Group 4 as authorized.

3. REPORT TITLE: Enter the complete report title in all capital letters. Titles in all cases should be unclassified. If a meaningful title cannot be selected without classification, show title classification in all capitals in parenthesis immediately following the title.

4. DESCRIPTIVE NOTES: If appropriate, enter the type of report, e.g., interim, progress, summary, annual, or final. Give the inclusive dates when a specific reporting period is covered.

5. AUTHOR(S): Enter the name(s) of author(s) as shown on or in the report. Enter last name, first name, middle initial. If military, show rank and branch of service. The name of the principal author is an absolute minimum requirement.

6. REPORT DATE: Enter the date of the report as day, month, year, or month, year. If more than one date appears on the report, use date of publication.

7a. TOTAL NUMBER OF PAGES: The total page count should follow normal pagination procedures, i.e., enter the number of pages containing information.

7b. NUMBER OF REFERENCES: Enter the total number of references cited in the report.

8a. CONTRACT OR GRANT NUMBER: If appropriate, enter the applicable number of the contract or grant under which the report was written.

8b, 8c, & 8d. PROJECT NUMBER: Enter the appropriate military department identification, such as project number, subproject number, system numbers, task number, etc.

9a. ORIGINATOR'S REPORT NUMBER(S): Enter the official report number by which the document will be identified and controlled by the originating activity. This number must be unique to this report.

9b. OTHER REPORT NUMBER(S): If the report has been assigned any other report numbers (*either by the originator or by the sponsor*), also enter this number(s).

10. AVAILABILITY/LIMITATION NOTICES: Enter any limitations on further dissemination of the report, other than those imposed by security classification, using standard statements such as:

- (1) "Qualified requesters may obtain copies of this report from DDC."
- (2) "Foreign announcement and dissemination of this report by DDC is not authorized."
- (3) "U. S. Government agencies may obtain copies of this report directly from DDC. Other qualified DDC users shall request through _____."
- (4) "U. S. military agencies may obtain copies of this report directly from DDC. Other qualified users shall request through _____."
- (5) "All distribution of this report is controlled. Qualified DDC users shall request through _____."

If the report has been furnished to the Office of Technical Services, Department of Commerce, for sale to the public, indicate this fact and enter the price, if known.

11. SUPPLEMENTARY NOTES: Use for additional explanatory notes.

12. SPONSORING MILITARY ACTIVITY: Enter the name of the departmental project office or laboratory sponsoring (paying for) the research and development. Include address.

13. ABSTRACT: Enter an abstract giving a brief and factual summary of the document indicative of the report, even though it may also appear elsewhere in the body of the technical report. If additional space is required, a continuation sheet shall be attached.

It is highly desirable that the abstract of classified reports be unclassified. Each paragraph of the abstract shall end with an indication of the military security classification of the information in the paragraph, represented as (TS), (S), (C) or (U).

There is no limitation on the length of the abstract. However, the suggested length is from 150 to 225 words.

14. KEY WORDS: Key words are technically meaningful terms or short phrases that characterize a report and may be used as index entries for cataloging the report. Key words must be selected so that no security classification is required. Identifiers, such as equipment model designation, trade name, military project code name, geographic location, may be used as key words but will be followed by an indication of technical context. The assignment of links, rules, and weights is optional.

PICATINNY ARSENAL TECHNICAL REPORT #255
..
**THE GRUNEISEN CONSTANT OF POROUS MATERIALS IN ENERGY
DEPOSITION MATERIALS**

BY

PAUL HARRIS

AUGUST 1971

Approved for public release - distribution unlimited.

**CONCEPTS AND EFFECTIVENESS DIVISION, NED
PICATINNY ARSENAL
DOVER, NEW JERSEY**

ACKNOWLEDGMENT

The author wishes to thank Mr. Louis Avrami of Picatinny Arsenal's Explosive Laboratory for suggesting the problem to him, and for many helpful discussions.

TABLE OF CONTENTS

	<u>PAGE NO.</u>
List of Illustrations	4
List of Tables	5
Abstract	6
Summary	7
Section	
I. Introduction	8
II. The Grüneisen Constant	10
III. Microscopic Effects and the Grüneisen Constant	13
IV. Shock Propagation in Porous Materials	19
V. Microscopic Effects on Shock Propagation	20
References	23
Distribution List	25

LIST OF ILLUSTRATIONS

<u>FIGURE NO.</u>		<u>PAGE NO.</u>
1	An Averaging Model for Effective Pressure Due to Energy Deposition in a Porous Solid	15
2	Shock Velocity versus Particle Velocity for Sintered Porous Copper	17
3	Model for a Porous Solid	19

LIST OF TABLES

<u>TABLE NO.</u>		<u>PAGE NO.</u>
I	Electron Mean Free Paths in Some Materials as a Function of Energy	11
II	Energy Deposition Properties of PETN	12
III	Grüneisen parameters for Sintered Porous Copper	18

ABSTRACT

It is proposed that the usual energy deposition, e.g., electron beam, experiments, as well as the usual shock introduction, e.g., flyer plate, experiments do not yield a true Grüneisen parameter of porous materials. It is proposed that in a porous material stress relief occurs within the time that energy is being deposited, or before the final state is reached in a flyer plate experiment. Both types of experiments are analyzed and correlated and agree with the ideas put forward here. Energy deposition experiments of Shea, Mazella, and Avrami (porous PETN), and flyer plate experiments of Boade (sintered porous copper), are considered.

Wave propagation in porous materials is considered in some detail, and it is concluded that in such materials macroscopic measurements can not always be used to determine microscopic parameters. It is proposed that a porous material acts as a diffraction grating with respect to a shock wave, and that unidirectional one-dimensional strain does not hold.

SUMMARY

In this report, we have looked at some of the details associated with shock propagation in porous materials. We have inquired into effects resulting from shock generation by "instantaneous" energy deposition or by shock introduction, e. g., via a flyer plate, at a free surface of the sample.

By considering the physics of energy deposition and shock propagation in a porous medium, we have shown that conventional techniques do not yield valid measurements of the true solid-state Grüneisen parameter, i. e., the relation between pressure and specific energy at constant volume, because on a microscopic scale determined by particle size, stress relief occurs before the final state is reached. This is true for the case of shock introduction and energy deposition. In the case of energy deposition, simple models which attempt to consider the result of stress relief within deposition time are presented. While the models are inadequate, they serve as a starting point for understanding the physics and for correlating the energy deposition and shock introduction cases.

Energy deposition experiments of Shea, Mazalle, and Avrami⁽¹⁴⁾, and shock introduction experiments of Boade⁽¹⁸⁾ are analyzed. In addition, we have applied some elementary considerations of a porous material as a diffractive medium to comment upon the difficulty of utilizing macroscopic experiments for investigating microscopic parameters. The difficulty being that local unidirectional one-dimensional strain cannot be assumed to hold. In this regard, we considered some flyer plate work in polyurethane as reported by Butcher⁽²¹⁾.

In the Introduction, we have considered the importance of porous materials from an academic and from an engineering point of view. Porous materials can be used for shock mitigation and/or as thermal standoff materials. Consequently, the U. S. Army and the shock wave community would like to understand as much as possible about porous solids. Considerable more work is needed.

L INTRODUCTION

Porous materials are any materials that happen to have a mass density less than the maximum possible equilibrium mass density at the pressure and temperature in question. Examples of such materials are foams, e. g., polyurethane, less than normal density explosives (1), and porous metals, e. g., porous tungsten (2).

Porous materials are of both engineering and academic interest. Polyurethane foams are utilized as shock mitigators by having the shock energy absorbed in the process of compacting the foam to its normal solid density. Porous metals have engineering applications but are also of extreme academic importance. If a solid of normal density is shock-loaded, its final state lies in a single curve (the Hugoniot curve) in the PV plane. On the other hand, when a solid such as porous tungsten is shock-loaded, the final state reached will reside on one of a continuum of Hugoniot curves, depending upon the initial porosity; the irreversible processes which occur during compacting yield PVT states for the compacted solid different from those occurring in the shock-loaded material having initial normal density. Thus, by shock-loading an initially porous material to beyond complete compaction, it is possible to investigate broad regions in PVT space. This academic property of porous materials was first pointed out by Zeldovich (3).

Another important application of porous materials is in the area of explosives. It is well known that the initiation sensitivity of explosives to mechanical shock depends upon the final density to which a granular explosive may be pressed (4). This area also has both academic and engineering applications.

Soviet and Western interest in inert porous materials, judging from the open literature, has been in different pressure regimes. Western interest⁺ (5, 6, 7, 8, 9) has been strong in the area of shock propagation in the pressure range at which compaction occurs. On the other hand, the Russians appear to have their main effort (2, 10, 11) in the pressure range beyond which compaction has already occurred. Among the interesting ingredients of high-pressure physics which the Russians have studied via porous materials is the electronic contribution to the Grüneisen constant (2).

There are two general ways by which porous materials may be examined experimentally. In one method, energy is dumped into the material in a very small time, more or less uniformly as a function of position and the shock effects accompanying the resulting thermal expansion may then be studied. A typical procedure for dumping in the energy utilizes an electron beam machine (12) which produces (typically), Mev

⁺The references in this report, for the most part, are meant to be illustrative rather than exhaustive.

electrons in large numbers within a pulse width from 20 nanoseconds to 70 nanoseconds. The electrons are scattered by the solid parts of the porous material, resulting in an increase in the internal energy of the material. The second general method involves the impacting of the porous material with a flyer plate⁽¹³⁾ of known mechanical properties. Instead of the shock originating within the material as in the energy dumping method, the shock now originates at the interface between the flyer and the sample target.

In this report, we wish to specifically consider an aspect of some electron beam experiments⁽¹⁴⁾ in porous samples of the explosive PETN (Pentaerythritol Tetra-nitrate). Some other experimental work will also be considered.

II. THE GRÜNEISEN CONSTANT

There are two possible definitions for the Grüneisen parameter, one microscopic, and the other macroscopic. The microscopic involves a model for interactions on an atomic level, while the macroscopic definition involves measurable parameters.

In the macroscopic definition, the Grüneisen constant, Γ , is defined by:

$$\Gamma = \frac{1}{\rho} \left(\frac{\partial p}{\partial E} \right)_{\rho} \quad (1)$$

where p is pressure, ρ is mass density, and E is internal energy[†]. Eq. (1) says that if one deposits thermal energy in a time small compared to the time necessary (defined below) for significant mass motion, then the pressure in the solid changes. The quantity Γ determines the change in pressure, and is a property of the structure of the material.

The time criteria mentioned above is usually taken as the time necessary for an acoustic wave to traverse an electron scattering mean free path in the solid. Let such a time be t_1 . If the pulse duration is T , then the constant volume definition of Eq. (1) requires:

$$T > t_1. \quad (2)$$

Physically, this means if Eq. (2) holds, then any energy inhomogeneities introduced by the electron beam are not relieved by acoustic signals before the energy is deposited. In other words, the energy can be considered as deposited instantaneously[§] if Eq. (2) holds.

[†]Actually, the Grüneisen parameter is a tensor quantity, and the stress tensor should be substituted for the pressure in Eq. (1). Such an anisotropy effect could be important in this report where we are interested in a pressure range comparable to the yield strength of the solid particles of PETN. Perhaps more important, the pressure range of interest is comparable to the pressure used in pressing the PETN to an initial density. Such pressing undoubtedly introduces anisotropy into the material which could conceivably show up in the experiment. In the Shea, Mazella, and Avrami experiment (14), peak pressures generated were in the one-kilobar range, while pressing pressures were in the one to ten-kilobar range. Because of a lack of sufficient experimental evidence to decide this question at the present time, we will assume here that Eq. (1) is correct in its present isotropic form.

[§]For those computer codes which can handle energy deposition and stress propagation simultaneously, T should be replaced in Eq. (2) by the time cycle. If the energy deposition is by other than electrons, the appropriate mean free path must be used. Since this report makes a point of physics, rather than technique, the possibility of handling hydrodynamics and energy deposition simultaneously is delayed until the discussion section of the report.

One of the main points of this report is that the time criteria of Eq. (2) is, in general, not valid for a porous material. All it takes to invalidate that criteria is that the average dimension of the solid particles making up the material be small compared to the appropriate radiation mean free path. For such small particles, the energy deposition-induced thermal stresses are relieved by thermal expansion prior to completion of the energy deposition process. Table I below lists some electron energy absorption mean free paths for a variety of materials and energies.

TABLE I		
ELECTRON MEAN FREE PATH AS A FUNCTION OF ENERGY		
Material	Mean Free Path	Electron Energy
Al	100 μ	0.4 Mev
PETN	500 μ	0.4 Mev
Be	1,000 μ	0.6 Mev
Quartz Crystal	4,000 μ	2 Mev
PETN	1,000 μ	4 Mev
Lead Styphnate	1,000 μ	4 Mev

As contrast to the typical dimension of $10^5 \mu$, i. e., 0.1 cm, of Table I, an acoustic wave propagating at 3×10^5 cm/sec can relieve the stress to the center of a 180μ particle in 30 nanoseccnds. Consequently, an electron beam machine having a pulse width of 30 nanoseconds (FWHM) would not be able to utilize the criteria of Eq. (2) for experiments with porous solids having particle sizes of 180μ or less. It is interesting to note that the 30-nanosecond figure is typical of the faster machines in use today. In the work by Shea, Mazella, and Avrami (hereafter called SMA), the average grain size of the PETN was observed to be 250μ . The electron beam was at 0.4 Mev with a pulse width of 25 nanoseconds (FWHM). Thus, if the PETN in question was porous enough so that a significant number of grains were not in intimate contact along a grain boundary, then the time criteria of Eq. (2) would be invalid.

We hasten to say that the work of SMA is still interesting in that it yields the magnitude of the pressure pulse resulting from a thermal energy deposition. Indeed, the experimenters were aware of the point with respect to time criteria made above at the time of their experiment, and that is why they speak in terms of an "effective" Grüneisen constant in their paper. The object now, however, is to see whether the measurements made can yield any useful information concerning microscopic processes. Table II lists the pertinent results of the SMA experiments.

TABLE II ^a			
ENERGY DEPOSITION PROPERTIES OF PETN			
ρ_{00}/ρ_0 ^b	Density gm/cm ³	Sound Speeds cm/sec $\times 10^{-5}$	Effective Γ
0.95	1.67	2.8	1.2
0.90	1.59	2.4 ± 0.1	0.51
0.87	1.54	1.8 ± 0.3	0.15
0.84	1.48	1.7 ± 0.3	(0.07 to 0.23)

^aThis table was taken, with minor changes, from reference 14.

^b ρ_0 denotes the normal density. ρ_{00} initial porous material density.

Although SMA report an experimental error in the measured Γ of 20 percent or more, the trend as a function of density is clearly discernible.

III. MICROSCOPIC EFFECTS AND THE GRÜNEISEN CONSTANT

In this section, we discuss some of the physics which might be important in interpreting the measured or effective Grüneisen constant. Integrating Eq. (1) gives⁺

$$P = \rho_i \Gamma (E - E_i) \quad (3)$$

where ρ_i denotes the initial density at which energy is deposited in the constant volume approximation, Γ is assumed independent of energy density, and E_i is the specific energy density prior to energy deposition. That Γ is indeed independent of E has been borne out experimentally by the success of the linear P vs E curve in fitting the data (14).

There are two relevant microscopic effects associated with the energy deposition aspect of porous solids. First, there is the possibility that surface energy effects, because of the large internal surface area expected in a porous solid, can play a role in determining the pressure, P . Second, is the expected and mentioned stress relief in the solid particles of the porous material.

Let us write (15) for the surface energy, γ_s :

$$\gamma_s = \frac{a_0 Y}{20} \quad (4)$$

where a_0 is the lattice parameter, and Y is Young's modulus for the solid particles. Using values for a typical solid:

$$Y = 10^{12} \text{ dynes/cm}^2, \quad a_0 = 2 \times 10^{-8} \text{ cm},$$

we find that:

$$\gamma_s = 10^3 \text{ ergs/cm}^2.$$

The heat of formation, $\Delta H_f = 5 \times 10^4$ cal/gram formula weight. For a solid of $\rho_0 = 5 \text{ gm/cm}^3$ and a gram formula weight of 50, we have an E_0 of:

$$E_0 = 5 \times 10^3 \text{ cal} \sim 2 \times 10^{11} \text{ ergs}$$

⁺In Eq. (3), we assume that the thermal pressures generated are considerably larger than the pressure before deposition, i. e., atmospheric pressure, and also larger than any internal stresses generated in the process of pressing the porous material to its initial density. There is a possibility that this last assumption is invalid since typical measured pressures (SMA) were in the fraction of a kilobar range, while pressing pressures were in the one to ten-kilobar range.

for one cm^3 of a typical solid. If the same cm^3 of material is now considered to have 10^3 cm^2 of internal surface area, S , (a factor of 10^3 more than external surface area):

$$\gamma_s S = 10^6 \text{ ergs.}$$

Comparison of E_0 and $\gamma_s S$ would seem to indicate that surface energy effects can be neglected. This view is further supported by the idea that surface energy is not expected to change during energy deposition; thermal expansion should allow stresses built up by deposition to be more or less instantly relieved so that neglecting temperature, the surface remains in a constant state.

Let P_1 denote the pressure in the normal density solid, and P_2 the pressure in the corresponding porous solid of initial density ρ_{00} :

$$P_1 \equiv p_0 \Gamma_1 (E - E_0) \quad (5a)$$

$$P_2 \equiv \rho_{00} \Gamma_2 (E - E_0) \quad (5b)$$

Since it has been shown that surface energy considerations are not important, the same specific internal energy has been used in Eqs. (5a) and (5b). Now let V_s be the volume occupied by the solid particles, and V_p that occupied by the voids. We wish to investigate the relation between Γ_1 and Γ_2 as a function of various models for averaging the pressure over the solid particles of the porous material. The averaging takes place with the mass motion frozen at the time at which energy deposition ends. One of the simplest averaging models is given by:

$$P_2^{(n)} \equiv P_1 \frac{V_s}{V_s + V_p}, \quad (6)$$

where $P_2^{(n)}$ simply denotes the pressure with this particular averaging model. Eq. (6) says that the pressure is reduced from that of the normal density solid by being smeared out over the entire volume to the solid particle. If m is the mass of the solid particle:

$$m = \rho_{00} (V_s + V_p) \quad (7a)$$

$$m = \rho_0 V_s \quad (7b)$$

$$\Gamma_2^{(n)} = \Gamma_1 \left(\frac{\rho_{00}}{\rho_0} \right)^{n-1} \quad (8)$$

Although the model given by Eq. (6) is unphysical, it is still interesting to note that it takes an exponent n greater than ten to fit the data of Table II, while $n = 1$ yields a Grüneisen parameter independent of porosity.

The next averaging model we consider is more physical and is shown in figure 1 following:

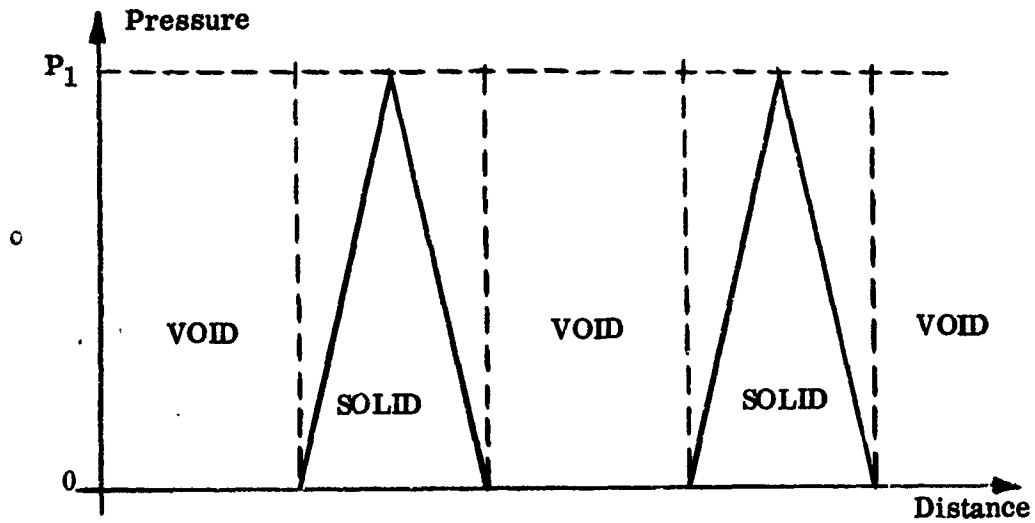


FIGURE 1: An Averaging Model for Effective Pressure Due to Energy Deposition in a Porous Solid

Averaging the pressure over the solid particles:

$$\bar{P}_2 = \frac{1}{(V_s + V_p)} \int_{V_s} P dV, \quad (9)$$

$$P = P_1 \left(1 - \frac{r^2}{a^2} \right), \quad (10)$$

where we are considering the particles to be spherical in Eq. (10). Using $V_s = \frac{4}{3} \pi a_s^3 = m/\rho_o$, we thus find:

$$\bar{P}_2 = \frac{P_1}{(V_s + V_p)} \int_0^{a_s} 4 \pi r^2 \left(1 - \frac{r^2}{a_s^2} \right) dr, \quad (11)$$

$$\bar{P}_2 = P_1 \frac{4 \pi}{(V_s + V_p)} \left[\frac{a_s^3}{3} - \frac{a_s^5}{5} \right] = \frac{2}{5} \left(\frac{\rho_{oo}}{\rho_o} \right) P_1 \quad (12)$$

$$\therefore \bar{\Gamma}_2 = \frac{2}{5} \Gamma_1. \quad (13)$$

The model leading to Eq. (13) is equivalent to assuming that a relief wave propagates toward the center of the particle, and that the wave decreases in amplitude as it propagates toward the particle center. It would also appear that a further assumption, that the wave just reaches the center of the particle at the end of the energy deposition, has been made. Once again, the averaging model is unphysical but interesting. We find an effective Grüneisen parameter which is dependent upon the spherical geometry, but independent of porosity. If anything, we have shown that the naive approaches will not work.

We feel that this type of work should be carried further. A more powerful and more physical approach than that presented above would use a computer program for stress wave analysis. The program would have to handle energy deposition and hydrodynamics at the same time (17). Having such a code, the proposal is then to look at the pressure time distribution in a slab of solid material, i. e., $\rho_0 = \rho_{00}$, where the slab is so thin that the acoustic transit time through it is small compared to the time associated with energy deposition.

There is a definite lack of data specifically relating to Grüneisen constant of porous materials before compaction occurs. It is possible, however, to analyze existing shock velocity versus particle velocity data to obtain such information. Figure 2 following, is based upon data taken from Boade (18) on sintered porous copper. If we let U_s be shock velocity, and u_p be particle velocity, then the extrapolations (dashed lines) in figure 2 can be represented by:

$$U_s = A + B u_p \quad (14)$$

Let Γ_0 be Grüneisen parameter corresponding to the extrapolated zero pressure state. It is easily shown (19) that:

$$\Gamma_0 = 2B - \frac{2}{3} \quad (15)$$

It is then a simple matter to apply Eq. (15) to figure 2.

For the data shown in figure 2, experimental points only exist for the 67.7 percent, 82.8 percent, and solid density sample. The other curves are theoretical. Applying Eq. (15) to the mentioned data gives the results shown in Table III.

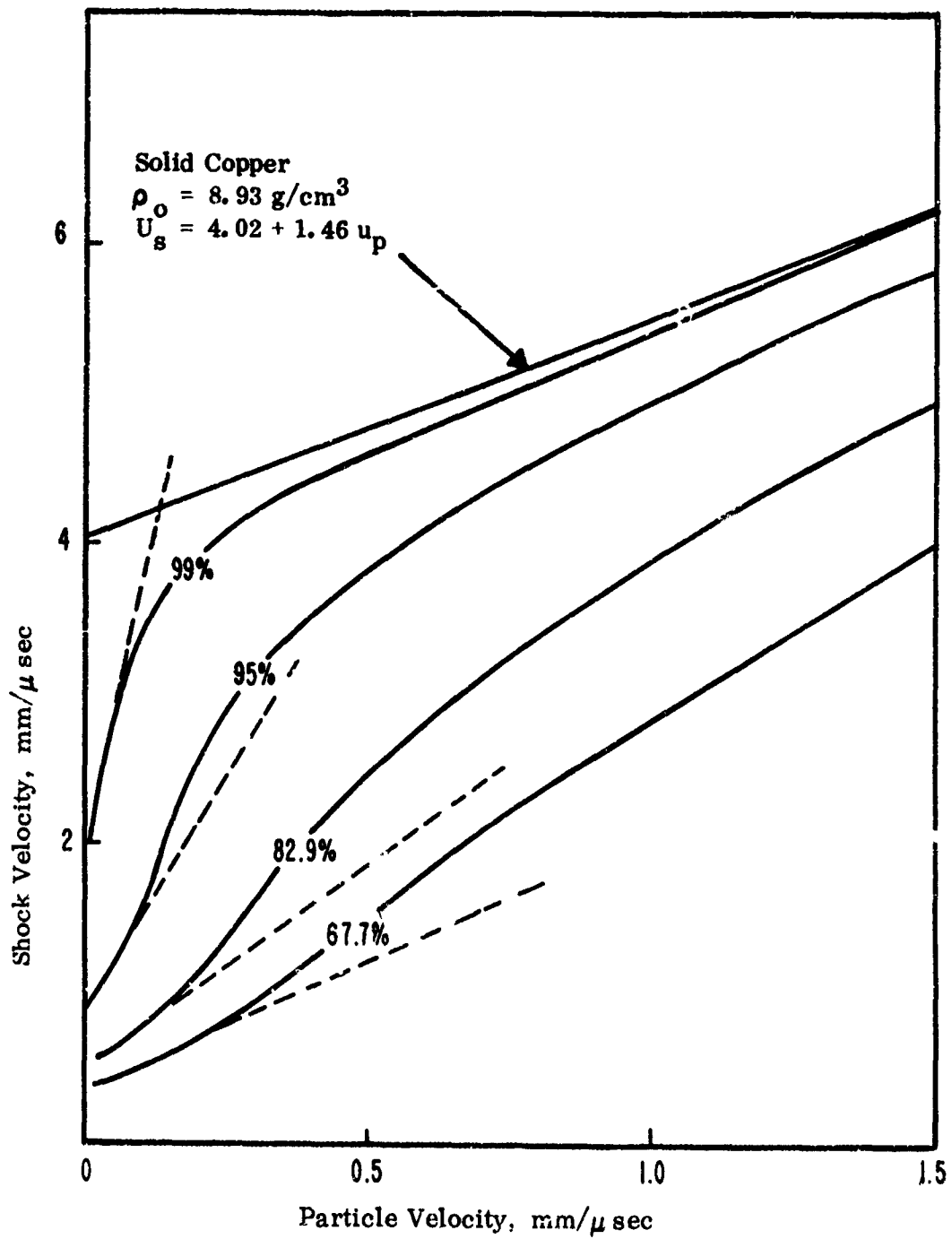


FIGURE 2: Shock velocity vs particle velocity for sintered porous copper (from Boade¹⁸). Percentage porosity is indicated by ρ_{00}/ρ_0 , and dashed lines are meant to extrapolate to zero pressure data.

TABLE III	
Grüneisen Parameter for Sintered Porous Copper	
ρ_{00}/ρ_c	Γ_0
0.677	2.79
0.829	4.67
1.00	2.25

The data thus show that the Grüneisen parameter decreases as the degree of porosity increases. This is similar to the averaging model of Eq. (8). On the other hand, the Γ_0 value corresponding to the solid density copper is lower than that of any of the experimentally observed porous density Γ_0 values. This last point is both unexpected and interesting. It correlates, however, with an observation made by SMA (14) that the calculated Grüneisen parameter for normal density, i. e., solid, PETN is 0.8 (with perhaps 20 percent error), which is smaller than the Γ associated with $\rho_{00}/\rho_0 = 0.95$, as shown in Table II. For the moment, this phenomenon is not understood.

IV. SHOCK PROPAGATION IN POROUS MATERIALS

In this section we would like to discuss the relationship between the Grüneisen data obtained from the impact experiments of Boade, and the energy deposition data obtained by SMA. We will then further discuss an aspect of the physics associated with shock propagation in porous materials.

Consider a porous material modeled as shown in figure 3:

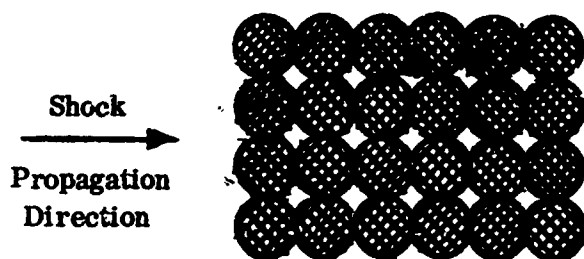


FIGURE 3: Model for a Porous Solid. (The shaded areas represent solid particles, and the unshaded areas are voids.)

If a shock of amplitude too small for compaction propagates into the material shown in figure 3, we first expect something akin to the Hugoniot state of a normal density solid to be transmitted across the contacting surfaces of the solid particles. The pressure corresponding to such a Hugoniot state would then be relieved in time by rarefactions entering the solid particles through their free surfaces. For solid particles with diameter small compared to the width of the shock front, the final state would thus be a function of the Hugoniot state in the normal state plus a relief factor.

Since the U_s versus u_p relation is measured for the final state, and thus so is the Grüneisen relation, the degree of porosity must play a role in determining Γ . Greater porosity means greater relief of the normal density pressure state, a reduced $\frac{\partial U_s}{\partial u_p}$ value, and thus a reduced Γ . The same physical phenomenon appears

to be occurring in the shock propagation determination of Γ as occurs in the energy deposition case.

V. MICROSCOPIC EFFECTS ON SHOCK PROPAGATION

An observer riding on a shock front in a porous material such as shown in figure 3 would see a succession of diffraction-grating planes. The effect of diffraction in general is to change the geometry of the wave front. In our case, the change is from plane wave geometry to nonplane wave geometry. Further specializing, we can say that on a microscopic particle size level, the mass disturbance is not unidirection one-dimensional strain* even though it may be unidirection one-dimensional strain on a macroscopic level. One-dimensional strain occurs when the dimensions of the sample perpendicular to the direction of shock propagation are large compared to the sample dimensions parallel to the direction of shock propagation. If the relative size of the dimensions are reversed, then the propagation is classified as one-dimensional stress. On a microscopic level, for spherical particles with some void separation between them as shown in figure 3, we thus expect a change in the geometry of the wave front.

If one is only interested in characterizing the macroscopic shock properties of a porous solid, then the unidirection one-dimensional strain view of the problem (with appropriate perpendicular and parallel dimensions) is valid. If, however, one wishes to use the data from the macroscopic experiment to determine microscopic parameters (such as a relaxation time), large errors could result. Physically, the reason for such errors is that diffraction modifies the way in which the principle of the conservation of momentum is applied.

In figure 4 following, we illustrate the result of microscopic diffraction. Originally, a plane wave is propagating in the z direction. After diffraction has occurred, small segment of the wave front, with area $(\Delta S)_\xi$ moves in the ξ direction (normal to the ξ axis).

*By one-dimensional strain we imply plane wave propagation with particle motion only in the direction of the wave propagation. The one-dimensional strain case is the typical configuration in shock wave theory and experiment.

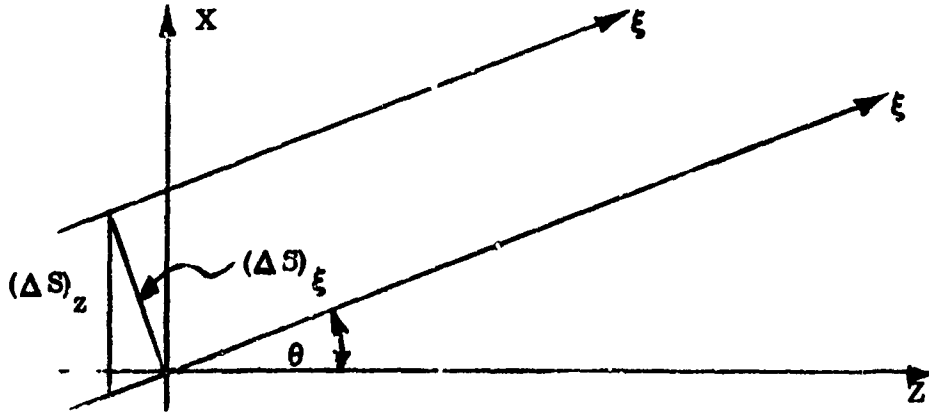


FIGURE 4: Diagram for Calculating the Results of Diffraction by Particle Structure in a Porous Solid

For brevity, assume that the local particle motion is also in the ξ direction. This simplification neglects the possibility of local transverse waves being generated due to the porous structure of the medium. In other words, we have local one-dimensional strain in other than the z direction. If π_{ξ} represents the momentum flux (20) in the ξ direction, then (20) :

$$\pi_{\xi} (\Delta S)_{\xi} = (p + \rho u_{\xi} u_{\xi}) (\Delta S)_{\xi}, \quad (16)$$

where p is pressure, ρ is mass density, and u_{ξ} the particle velocity in the ξ direction.

$$(\Delta S)_{\xi} = (\Delta S)_z \cos \theta \quad (17)$$

Let \dot{P}_z be the momentum transferred per time across $(\Delta S)_z$.

$$\dot{P}_z \equiv \pi_z (\Delta S)_z = \dot{P}_{\xi} \cos \theta \quad (18)$$

$$\therefore \dot{P}_z = \pi_{\xi} (\Delta S)_{\xi} \cos \theta \quad (19)$$

$$\therefore \pi_z = (p + \rho u_{\xi} u_{\xi}) \cos^2 \theta, \quad (20)$$

or

$$\pi_z = p \cos^2 \theta + \rho u_z u_z. \quad (21)$$

Two points now need to be made. First, when employing the conservation of momentum in shock wave problems, people usually equate the right hand side of Eq. (21) on each side of the shock front (with $\theta=0$). Second, even though no net deviation from macroscopic one-dimensional strain in the z direction is observed, a nonzero average value for $\cos^2 \theta$ is expected to exist.

Butcher⁽²¹⁾ uses Eq. (20) with $\theta = 0$ to investigate shock propagation in 0.96 gm/cc polyurethane foam. He was interested in the relaxation time, τ_0 , for void collapse (closure) and generated an equation of the form:

$$u_z = \frac{A (\sigma - \sigma_{eq}) / \tau_0}{(B + C \sigma)} \quad (22a)$$

where A, B, and C may be regarded here as constants. Our point is that an equation more in the form of:

$$u_z = \frac{A (\sigma - \sigma_{eq}) \overline{\cos^2 \theta} / \tau_0}{(B + C \sigma \overline{\cos^2 \theta})} \quad (22b)$$

should have been used. In Eqs. (22), σ denotes stress, σ_{eq} an equilibrium stress value, and $\overline{\cos^2 \theta}$ an average value of $\cos^2 \theta$. Such a correction, at least in the numerator of Eq. (22b), would result in a larger value of τ_0 than previously estimated. A larger value of τ_0 would be in keeping with some other ideas (based upon a "simplified gap model") put forward by Butcher⁽²¹⁾. At the moment, we do not have a good model for calculating $\overline{\cos^2 \theta}$.

REFERENCES

1. V. A. Vasil²ev et al, Combustion, Explosion, and Shock Waves 3, 371 (1967).
2. K. K. Krupnikova, Soviet Physics - JETP 15, 470 (1962).
3. Ya. B. Zel'dovich, Soviet Physics - JETP 5, 1103 (1957).
4. M. W. Evans et al, Fourth Symposium on Detonation, 12-15 October 1965, White Oak, Silver Spring, Maryland, p 359.
5. J. Thouvenin, Fourth Symposium on Detonation, 12-15 October 1965, White Oak, Silver Spring, Maryland p 258.
6. H. P. Lavender, Theoretical-Experimental Correlation of Large Explosively-Induced Transient Deformations of Polyurethane Foam Metal Slabs, Air Force Dynamics Laboratory, Wright-Patterson Air Force Base, Ohio. AFFDL-TR-67-106, AD822911, dated September 1967.
7. B. M. Butcher and C. H. Kannes, Dynamic Compaction of Porous Iron, Sandia Laboratories, Albuquerque, New Mexico, SC-R 67-3040, dated April 1968.
8. W. Hermann, Journal of Applied Physics 40, 249 (1969).
9. J. Seaman and R. K. Linde, Distended Material Model Development, Vol. 1, Stanford Research Institute, Menlo Park, California, Contract No. F29601-67-C-0073, Report No. AFWL-TR-68-143, Vol. 1, dated May 1969.
10. S. B. Kormer et al, Soviet Physics JETP 15, 447 (1962).
11. V. N. Zharkov and V. A. Kalinin, Equations of State for Solids at High Pressures and Temperatures (Consultants Bureau, New York, 1971).
12. R. A. Graham and R. E. Hutchison, Applied Physics Letters 11, 69 (1967).
13. For a general review of flyer plate technology see, for example, H. M. Berkowitz and L. J. Cohen, A Study of Plate Slap Technology, Part I, McDonnell-Douglas Astronautics Company, Huntington Beach, California, Report No. AFML-TR-69-106, Part I, dated June 1969.
14. J. H. Shea, A. Mazella, and L. Avrami, Fifth Symposium on Detonation, Pasadena, California, 18-21 August 1970.

REFERENCES (Continued)

15. A. S. Tetelman and A. J. McEvily, Jr., Fracture of Structural Materials, (John Wiley and Sons, Incorporated, New York, 1967).
16. D. R. Stull and G. C. Sinke, Thermodynamic Properties of the Elements (American Chemical Society, Washington, D. C. 1956).
17. The PUFF V-EP Code of Kaman Nuclear Corporation does handle such problems.
18. R. R. Boade, Experimental Shock Loading Properties of Porous Materials and Analytic Methods to Describe These Properties, Sandia Laboratories, Albuquerque, New Mexico, Report SC-DC-70-5052, dated 1970.
19. Y. K. Huang, Journal of Chemical Physics 51, 2573 (1969).
20. L. D. Landau and E. M. Lifshitz, Fluid Mechanics (Addison-Wesley, New York, 1969), Section 7.
21. B. M. Butcher, The Description of Strain Rate Effects in Shocked Porous Materials, Seventh Sagamore Army Materials Research Conference, Raquette Lake, New York, dated September 1970.